Available online www.jsaer.com

***Journal of Scientific and Engineering Research*, 2017, 4(1):135-145**

Research Article

ISSN: 2394-2630
CODEN(USA): JSERBR

3D Study of a Bifacial Polycrystalline Silicon Solar Cell Back Surface Illuminated: Influence of Grain Size and Recombination Velocity

Moustapha THIAME[1], Alassane DIENE[2], Boureima SEIBOU[3], Cheikh Tidiane SARR[1], Mohamed Lemine OULD CHEIKH[1], Ibrahima DIATTA[1], Mayoro DIEYE[1], Youssou TRAORE[1], Gregoire SISSOKO[1]

[1]Laboratoire des Semi-conducteurs et d'Energie Solaire, Faculté des Sciences et Techniques, Université Cheikh Anta Diop, Dakar, Sénégal
[2]Ecole Polytechnique de Thiès, Thiès, Sénégal
[3]Ecole des Mines de Niamey Niger

Abstract Calculation was carried out by solving minority carrier continuity equation in the base of solar cell back illumited with white light .The physical parameters that influence the solar cell performance are geometric (H, g) and electronic (Sf, Sb, Sg). Mathematical correlations are established among these parameters to optimize the solar cell response.

Keywords solar cell, carrier density, current density, photovoltage, recombination velocity, grain size

1. Introduction

Solar cell works for improving efficiency are diverse [1-2]. The theoretical modeling related to experimental studies focus on physical phenomena that govern the solar cell operation [3-5].

This is the generation - recombination and diffusion of photocreated minority charge carriers in the solar cell consisting essentially of 3 parts: the emitter, the space charge region and the base [6] and their boundary surfaces.

Both experimental [7] and theoretical [8] studies are based on a one-dimensional or three-dimensional geometric forms [9].

The one-dimensional model reveals the physical mechanisms at the junction, in volume and at back surface [10].

The three-dimensional model reveals recombination at grain boundaries by focusing on grain size and at grain boundaries recombination [11-12].

The theoretical choices are based on diffusion equation resolution of minority carrier taking into account the operating regime: static regime [13-16], transient dynamic regime [17-18] or dynamic frequency regime [19-20].

The solar cell system geometry is great importance because the objective is to create maximum carriers near the space charge region (SCR) [21]. Then the choice of illumination from either front or back side of the cell [22] or both side simultaneously [23] are proposed. Other geometries such as junction vertical parallel solar cell and series [24] make it possible to bring the collecting surface closer to the photogenerated carriers.

Our study focuses on a rear-illuminated solar cell [25] to highlight the effect of recombination at grain boundaries, grain size, and recombination velocity on the back side Sb, on the electrical parameters.

2. Modeling and Theoretical Analysis

In this study, we use n^+ - p - p^+ type of a bifacial polycrystalline silicon solar cell. Silicon consisting of several grain of various sizes, for our study, we use the 3D columnar model where each grain has a rectangular shape as shown in Figure 1 below [3,6,12, 22].

A 3D mark is placed at the center at the space charge region.

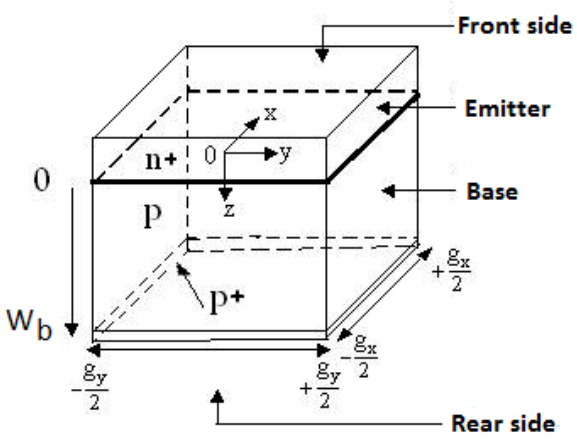

Figure 1: Polycrystalline silicon columnar grain model

In this study, the contribution of the emitter is neglected [3, 12]. We take into account only the base contribution.

In addition, it is considered that the illumination applied to the rear side of the solar cell is uniform, which then provides a generation rate that depends only on z, the base depth [23]. Finally, we considered that the existing crystalline field within the base is neglected and recombination velocity at the grain boundaries is perpendicular to the junction and independent to the generation rate under AM 1.5 [3, 15, 25].

2.1. Density of Minority Carriers in the Base

When the solar cell is illuminated by the rear side with a constant multispectral light, the minority carriers density in the base is governed by the following continuity equation:

$$\frac{\partial^2\delta(x,y,z)}{\delta x^2}+\frac{\partial^2\delta(x,y,z)}{\partial y^2}+\frac{\partial^2\delta(x,y,z)}{\delta z^2}=\frac{\delta(x,y,z)}{L^2}-\frac{1}{D}\sum_{i=1}^{3}a_i\cdot\exp(-b_i\cdot(wb\cdot z)) \quad (1)$$

with L: diffusion length; D: diffusion coefficient; a_i and b_i are the tabulated values of solar radiation and the dependence of silicon absorption coefficient with wavelength for AM = 1.5 [26-27].

The resolution of the continuity equation (1) taking into account boundary conditions namely recombination at grain boundaries, recombination on the back surface and at the junction, allows us to obtain the expression of the carrier density.

A general solution to this equation can be written as follows [3, 28]:

$$\delta(x,y,z)=\sum_k\sum_j Z_{k,j}(z)\cdot\cos(c_k x)\cos(c_j y) \quad (2)$$

The terms c_k and c_j are obtained using the following boundary conditions at the grain boundaries [3, 11, 25]:

$$\left[\frac{\partial\,\delta(x,y,z)}{\partial x}\right]_{x=\pm\frac{gx}{2}}=\mp\frac{Sgb}{D}\cdot\delta(\pm\frac{gx}{2},y,z) \quad (3)$$

$$\left[\frac{\partial\,\delta(x,y,z)}{\partial y}\right]_{x=\pm\frac{gx}{2}}=\mp\frac{Sgb}{D}\cdot\delta(x,\pm\frac{gy}{2},z) \quad (4)$$

- S_{gb} is the recombination velocity at grain boundaries. It allows expressing the

recombination rate of minority charge carriers at grain boundaries.
- gx and gy are grain sizes according to x and y axes.
From equations 3 and 4, we get the following transcendental equations systems:

$$c_k \cdot \tan(c_k \cdot \frac{gx}{2}) = \frac{Sgb}{D} \quad (5)$$

$$c_j \cdot \tan(c_j \cdot \frac{gy}{2}) = \frac{Sgb}{D} \quad (6)$$

The solutions of equations 5 and 6 are obtained by a graphic resolution instead of numericcal one.

Using the orthogonality of $\cos(c_k x)$ and $\cos(c_j y)$ functions, we obtain the $Z_{k,j}(z)$ expression as:

$$Z_{k,j}(z) = M_{k,j} \cdot ch(\frac{z}{L_{k,j}}) + N_{k,j} \cdot sh(\frac{z}{L_{k,j}}) - \sum_{i=1}^{3} K_i \cdot \exp(-b_i \cdot (wb \cdot z)) \quad (7)$$

with $L_{k,j} = \left[c_k^2 + c_j^2 + L^{-2}\right]^{-\frac{1}{2}}$ (8)

$$K_i = \frac{L_{k,j}^2}{D_{k,j} \cdot \left[b_i^2 \cdot L2_{k,j} - 1\right]} \cdot a_i \quad (9)$$

$$D_{k,j} = \frac{D \cdot \left[\sin(c_k \cdot gx) + c_k \cdot gx\right] \cdot \left[\sin(c_j \cdot gy) + c_j \cdot gy\right]}{16 \cdot \sin(c_k \cdot \frac{gx}{2}) \cdot \sin(c_j \cdot \frac{gy}{2})} \quad (10)$$

The constants $M_{k,j}$ and $N_{k,j}$ are obtained with the boundary conditions at the junction and at the back surface which are [10, 29-30]:

$$\left[\frac{\partial \delta(x,y,z)}{\partial z}\right]_{z=0} = \frac{Sf}{D} \cdot \delta(x,y,0) \quad (11)$$

$$\left[\frac{\partial \delta(x,y,z)}{\partial z}\right]_{z=wb} = -\frac{Sb}{D} \cdot \delta(x,y,wb) \quad (12)$$

In these expressions, Sf represents the minority carrier recombination velocity at the junction which reflects the flow of carriers crossing the junction and Sb is the recombination velocity on the back surface. It allows expressing how minority carriers in the base disappear to the back side.

$$M_{k,j} = \sum_{k=1}^{3} K_i \cdot \frac{\frac{1}{L_{k,j}} \cdot (\frac{Sb}{D} + b_i) + Y_{k,j} \cdot (\frac{Sf}{D} - b_i) \cdot \exp(-b_i \cdot wb)}{\frac{Sf}{D} \cdot Y_{k,j} + \frac{X_{k,j}}{L_{k,j}}} \quad (13)$$

$$N_{k,j} = \sum_{i=1}^{3} K_i \cdot \frac{\frac{Sf}{D} \cdot (\frac{Sb}{D} + b_i) - X_{k,j} \cdot (\frac{Sf}{D} - b_i) \cdot \exp(-b_i \cdot wb)}{\frac{Sf}{D} \cdot Y_{k,j} + \frac{X_{k,j}}{L_{k,j}}} \quad (14)$$

with : $X_{k,j} = \frac{1}{L_{k,j}} \cdot sh(\frac{wb}{L_{k,j}}) + \frac{Sb}{D} \cdot ch(\frac{wb}{L_{k,j}})$ et $Y_{k,j} = \frac{1}{L_{k,j}} \cdot ch(\frac{wb}{L_{k,j}}) + \frac{Sb}{D} \cdot sh(\frac{wb}{L_{k,j}})$ (15) and (16)

2.2. Photocurrent Density

The photocurrent density is obtained from the expression of the minority carriers density in the base. It is given by [3, 6, 13, 25, 29] :

$$J = \frac{q \cdot D}{gx \cdot gy} \int_{-\frac{gx}{2}}^{+\frac{gx}{2}} \int_{-\frac{gy}{2}}^{+\frac{gy}{2}} \left[\frac{\partial \delta(x,y,z)}{\partial z}\right]_{z=0} \cdot dx \cdot dy \quad (17)$$

After calculation we get:

$$J = q \cdot D \cdot \sum_k \sum_j R_{k,j} \cdot \left(\frac{N_{k,j}}{L_{k,j}} - \sum_{i=1}^{3} K_{k,j} \cdot b \cdot \exp(-b \cdot wb) \right) \quad (18)$$

$$\text{with } R_{k,j} = \frac{4 \cdot \sin(\frac{c_k \cdot gx}{2}) \cdot \sin(\frac{c_j \cdot gy}{2})}{gx \cdot gy \cdot c_k \cdot c_j} \quad (19)$$

2.3. Photovoltage

It is obtained using the Boltzmann expression [3, 25, 29]

$$V = V_T \cdot \log\left[1 + \frac{N}{n_i^2} \cdot \int_{-\frac{gx}{2}}^{+\frac{gx}{2}} \int_{-\frac{gy}{2}}^{+\frac{gy}{2}} \delta(x, y, 0) \right] \quad (20)$$

This leads to:

$$V = V_T \cdot \ln\left(1 + \frac{N}{n_i^2} \cdot \sum_k \sum_j R_{k,j} \left[M_{k,j} - \sum_{i=1}^{3} K_{k,j} \cdot \exp(-b_i \cdot wb) \right] \right) \quad (21)$$

3. Results and Discussion

3.1. Study of the Minority Carriers Density in the Base

Are presented in Figures 2 and 3 the profiles of the excess minority carriers density as a function of base depth, respectively for different recombination velocities at the grain boundaries and for different grain sizes.

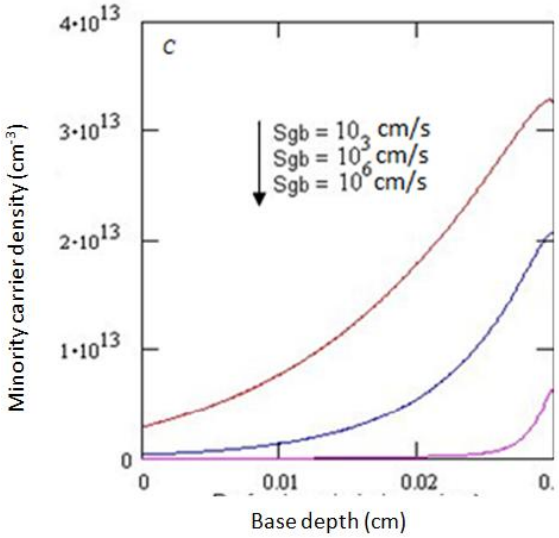

Figure 2: Profile of the excess minority carrier density as a function of depth z in the base for different Sgb ; g=0.005cm, $Sf = 3.10^3 cm/s$, $Sb = 3.10^3 cm/s$ $wb = 0.03cm$ and AM1.5

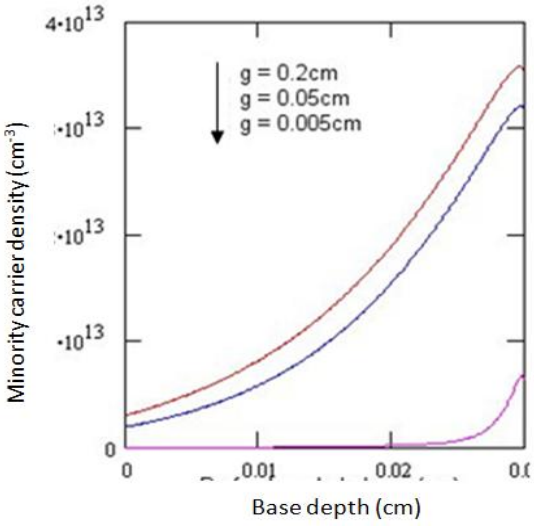

Figure 3: Profile of the excess minority carrier density as a function of depth z in the base for different grain sizes; $Sgb = 10^5 cm/s$; $Sf = 3.10^3 cm/s$, $Sb = 3.10^3 cm/s$; and AM1.5.

These profiles show that the density of minority carriers in the base increases as one approaches the back. This is related to the generation rate which decreases exponentially as the distance from the back side along the axis z increases. The number of carriers generated is also much higher in the back than in the front [23] (Fick law). The analysis of the curves shows that the decrease in the grain size causes a decrease of the carrier density [13, 28-29]. Indeed, the reduction in grain size leads to an increase of recombination centers at the grain boundaries. We also note that the higher the recombination rate at the grain boundaries, the more the carrier density is small. This change highlights the effect of recombination at the joints.

3.2. Study of the Photocurrent Density

Figures 4 and 5 show the profiles of the photocurrent density as a function of the recombination velocity at the junction, respectively for different grain sizes and different recombination velocities at the grain boundaries.

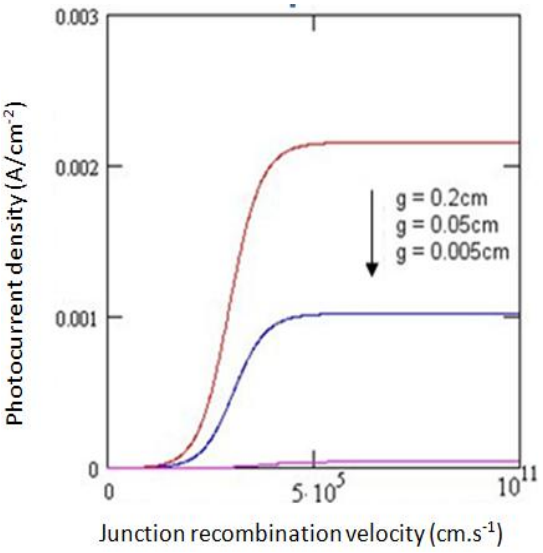

Figure 4: Profile of the photocurrent density as a function of the recombination velocity at the junction for different grain sizes; $b = 10^5 cm/s$; $Sb = 3.10^3 cm/s$; $wb = 0.03cm$ *and AM1.5*

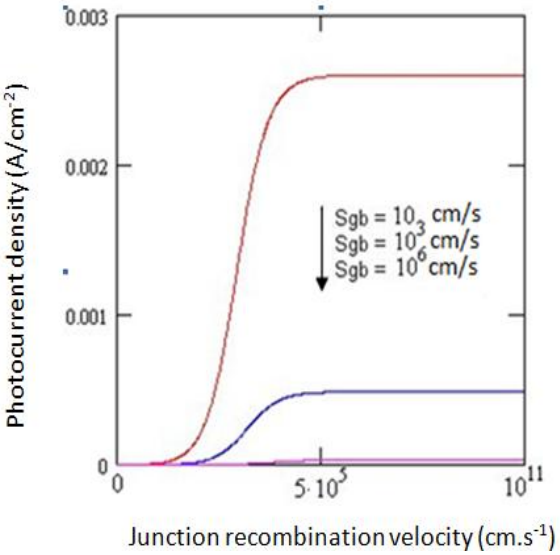

Figure 5: Profile of the excess minority carriers density, based on the recombination velocity at the junction for different Sgb; g=0.005 cm; $Sb = 3.10^3 cm/s$, $wb = 0.03cm$ *and AM1.5*

The profiles show that the photocurrent density is almost zero for low recombination velocity values at the junction (Sf ≤ 2.10^2cm/s), which corresponds to an open circuit mode of the solar cell. It gradually increases with Sf when 2.10^2cm/s ≤ Sf ≤ 5.10^5cm/s and becomes constant for Sf ≥ 5.10^5 cm/s. In the latter area, the solar cell is in short-circuited mode.

In this area, the photocurrent density decreases almost by 50% when the grain size passes from 0.2 cm to 0.005cm. It becomes almost zero when the grain size approaches 0.005cm. It decreases by about 80% when the recombination velocity at grain boundaries ranges from 10 cm/s to 10^3 cm/s.

For very high recombination velocities (6.10^6 cm / s), the photocurrent density tends to zero.

Therefore these figures highlight the discreasing of the photocurrent density when the recombination rate is important in the base substrate of the solar cell.

3.3. Study of the Short Circuit Current Density

We get the short-circuit current density Jsc from the photocurrent density for large values of the recombination velocity at the junction [10, 29].

It is given by the expression

$$Jsc = \lim_{Sf \geq 5.10^5 cm/s} J \qquad (22)$$

Expression of the short circuit current density for an illumination of the solar cell from the back side is given by equation (23) below:

$$Jcc = q \cdot D \cdot \sum_k \sum_j \frac{R_{k,j}}{L_{k,j}} \cdot \sum_{i=1}^{3} K_{k,j} \cdot \left(\frac{1}{Y_{k,j}} \cdot \left(\frac{Sb}{D} + b_i \right) - \left(\frac{X_{k,j}}{Y_{k,j}} + b_i \cdot L_{k,j} \right) \cdot \exp\left(-b_i \cdot wb \right) \right) \qquad (23)$$

To assess the effect of grain size and the recombination velocity at the joints on the short-circuit current density, we represent in the Figure 6 the profile according to the recombination velocity at the grain boundaries for different size grain, and in Figure 7 the profile according to the grain size for different recombination velocities at the grain boundaries.

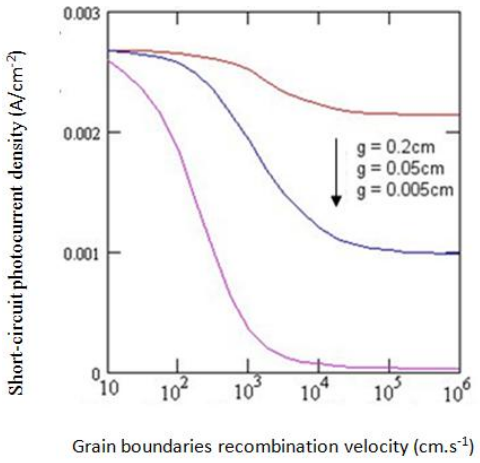

Figure 6: Profile of the short-circuit current density according to the recombination velocity at the grain boundaries for different grain size with $Sb = 3.10^3 cm/s;\ wb = 0.03cm$ *and AM1.5.*

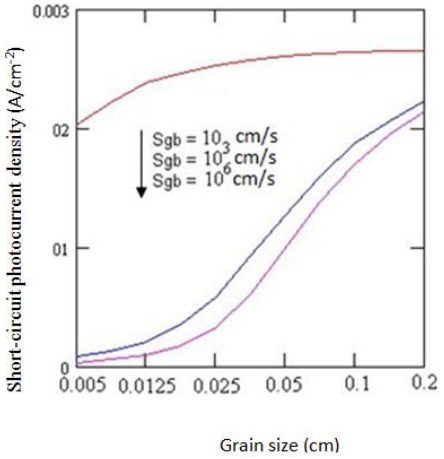

Figure 7: Profile of the short-circuit current density according to the grain size for different recombination velocities at the grain boundaries with, $b = 3.10^3 cm/s;\ wb = 0.03cm$

Analysis of the curves shows that the short circuit current density generally decreases as the recombination velocity at grain boundaries increases, and more the grain size is small, the more it is low. Recombination at grain boundaries has a powerful influence on the short-circuit current when the grain size is small.

For high grain size and low recombination velocities, the short-circuit current is almost constant and is substantially equal to that delivered by a monocrystalline solar cell illuminated by the back side [6, 13, 28-29].

3.4. Study of the Photovoltage

Figures 4 and 5 show the profiles of the photocurrent density as a function of the recombination velocity at the junction, respectively for different grain size and different recombination velocities at the grain boundaries [3, 6, 25, 29].

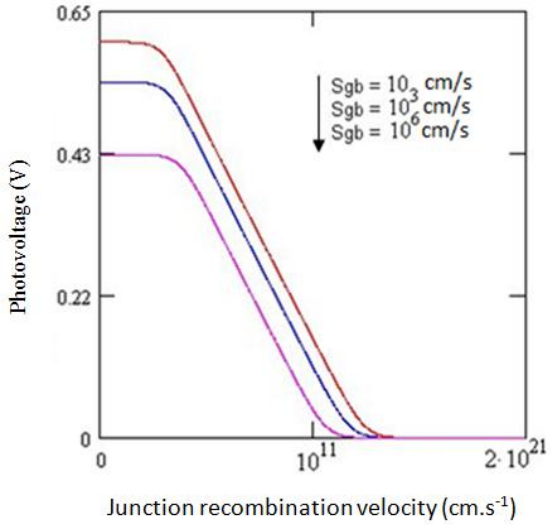

Figure 8: Profile of the photovoltage density, as a function of the recombination velocity at the junction for different recombination velocities at the grain boundaries: g=0.005 cm, $Sb = 3.10^3 cm/s\ \ wb = 0.03cm$ *and AM1.5.*

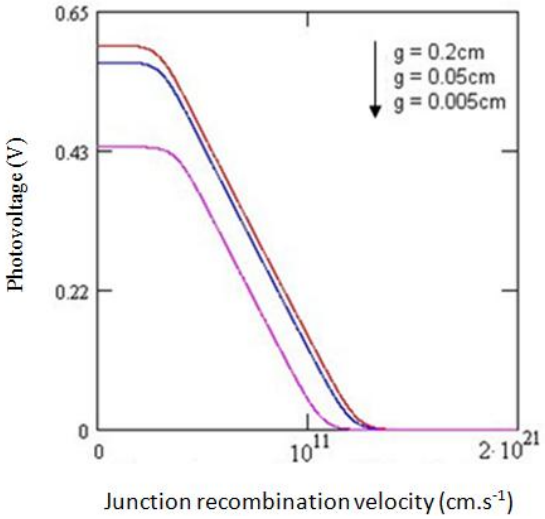

Figure 9: Profile of the photocurrent density as a function of the recombination velocity at the junction for different grain sizes: $Sgb = 10^5 cm/s;\ Sb = 3.10^3 cm/s\ \ wb = 0.03cm$ *and AM1.5.*

The profiles show that the photovoltage has a horizontal bearing for low values of the recombination velocity at the junction ($Sf \leq 3.10^3$cm / s), which corresponds to the solar cell operation in open circuit; then it decreases when Sf increases.

It generally decreases when the recombination rate at the grain boundaries increases and when the grain size decreases.

3.5. Study of the Photovoltage in Open Circuit Condition

In open circuit condition, the recombination velocity at the junction tends to zero, so we get the expression of the open circuit photovoltage in exploiting the following equation [29]:

$$Vco = V(Sf \leq 3.10^3 \text{cm / s}) \quad (24)$$

which gives:

$$Vco = V_T \cdot \ln\left(1+\frac{N}{n_i^2}\sum_k\sum_j R_{k,j}\cdot\sum_{i=1}^{3}K_{k,j}\cdot\left[\frac{1}{X_{k,j}}\cdot\left(\frac{Sb}{D}+b_i\right)-\left(\frac{Y_{k,j}}{X_{k,j}}\cdot b_i\cdot L_{k,j}+1\right)\cdot\exp(-b_i\cdot wb)\right]\right) \quad (25)$$

To assess the effect of grain size and recombination at the joints on the voltage in open circuit, we represent in figure 10 the profile according to the recombination velocity at the grain boundaries for different grain size and in figure 11, its profile as a function of the grain size for different recombination velocities at the grain boundaries.

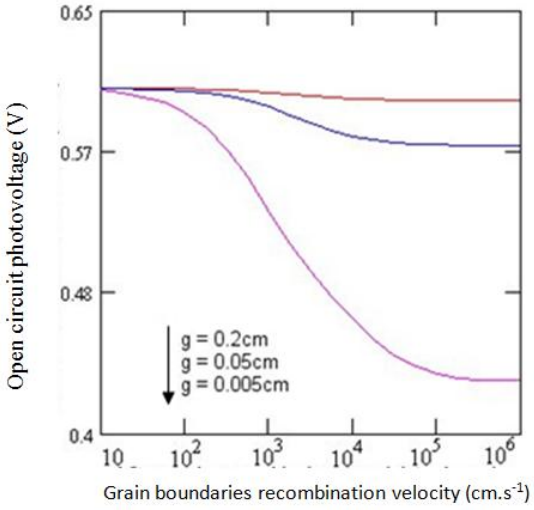

Figure 10: profile of photovoltage density in open-circuit condition, depending on the recombination velocity at grain boundaries for different grain sizes, $Sb = 3.10^3 cm/s$; wb=0.03cm and AM1.5.

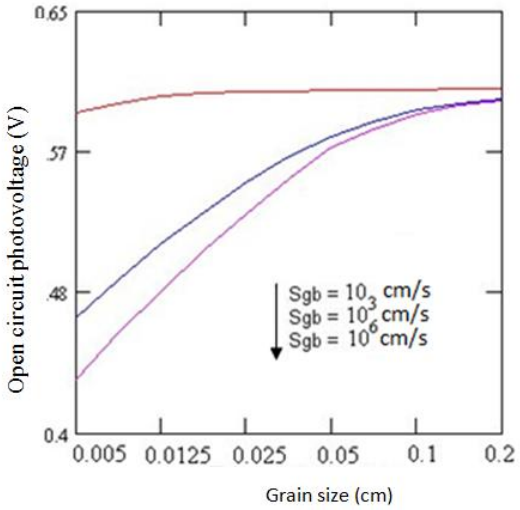

Figure 11: Profile of photovoltage density in open circuit condition, depending on the grain size for different recombination velocities at the grain boundaries; $Sf = 3.10^3 cm/s$; $Sb = 3.10^3 cm/s$ wb=0.03cm and AM1.5.

For Figure 10, the analysis of the curve shows that the photovoltage which is plotted as a function of the recombination velocity at the grain boundaries decreases and generally decreases as the grain size decreases. Analysis of Figure 11 shows that the photovoltage which is plotted versus the grain size increases and generally decreases as the recombination velocity at the grain boundaries increases.

The influence of the recombination velocity at grain boundaries on the open circuit photovoltage is more remarkable when the grain size is small.

This confirms that the presence of crystals of small grain sizes in the Si material corresponds to an increase of recombination centers.

3.6. Current - voltage characteristics

The current - voltage characteristic is obtained by plotting the current density provided as a function of the photovoltage linked by Sf [31].

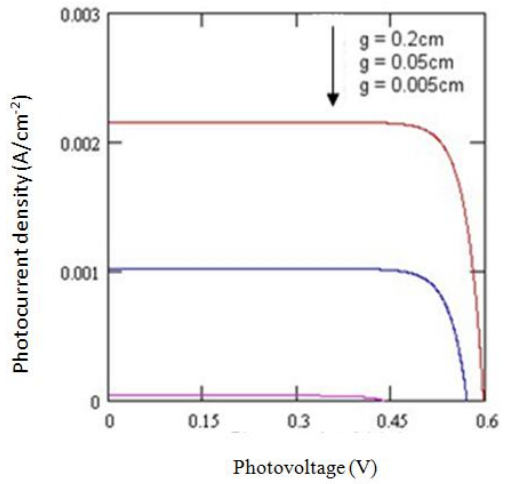

Figure 12: current-voltage characteristic for different grain sizes with $b = 10^5 cm/s$, $Sb = 3.10^3 cm/s$; *wb*=0.03*cm and AM1.5.*

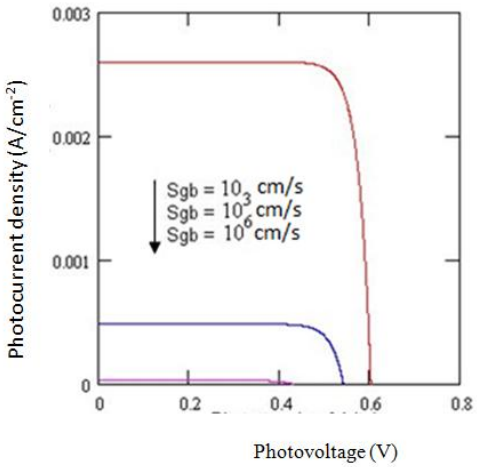

Figure 13: current - voltage characteristic for different values of Sgb , *g=0.005cm and for,* $Sb = 3.10^3 cm/s$, *wb*=0.03*cm and AM1.5*

The analysis of the curves shows that the current - voltage characteristic generally decreases when the recombination velocity at the grain boundaries increases and when the grain size decreases [28, 29]. When the photovoltage is zero, the photocurrent corresponds to the short-circuit current and when the current goes to zero, the voltage is the open circuit voltage.

The decrease in the short circuit current rating is more than 50% when the grain size decreases from 0.2 cm to 0.05 cm. It tends to zero when the grain size becomes very small (0.005cm).

3.7. Recombination Parameter: Recombination Velocity on the Back Side Sb

When the solar cell is illuminated from the back side, strong recombination of photocreated carriers is observed. The control of back side recombination parameter could be useful to improve the quality of these solar cells. To determine the back surface recombination velocity, we consider that the current density is the sum of many small current densities: the $J_{k,j}$ depending on solutions of transcendental equations (5) and (6) [6,13,29].

$$J = \sum_k \sum_j J_{k,j} \tag{26}$$

With: $$J_{k,j} = q \cdot R_{k,j} \cdot Sf \cdot \sum_{i=1}^{3} K_{k,j} \cdot \frac{\frac{Sb - D \cdot b_i}{D \cdot Y_{k,j}} \cdot \exp(-b_i \cdot wb) - \frac{X_{k,j}}{Y_{k,j}} + b_i \cdot L_{k,j}}{\frac{X_{k,j}}{Y_{k,j}} + \frac{Sf \cdot L_{k,j}}{D}} \tag{27}$$

The current density being constant for very large junction recombination velocity Sf values [10, 29].

We can then write: $$\left(\frac{\partial J}{\partial Sf}\right)_{Sf \geq 5.10^5 cm/s} = 0 \tag{28}$$

This allows us to have $Sb_{k,j}$ expression, a recombination velocity which depends on c_k , c_j , solutions of transcendental equations (5) and (6).

$$Sb_{k,j} = \frac{D}{L_{lk,j}} \cdot \frac{\sum_{i=1}^{3} K_i \cdot \left[\left(\sinh(\frac{wb}{L_{k,j}}) + b_i \cdot L_{k,j} \cdot \cosh(\frac{wb}{L_{k,j}})\right) \cdot \exp(-b_i \cdot wb) - b_i \cdot L_{k,j}\right]}{\sum_{i=1}^{3} K_i \cdot \left[1 - \left(\cosh(\frac{wb}{L_{k,j}}) + b_i \cdot L_{k,j} \cdot \sinh(\frac{wb}{L_{k,j}})\right) \cdot \exp(-b_i \cdot wb)\right]} \tag{29}$$

We have a new expression that describes how the minority carriers in the base recombine when the solar cell is illuminated from the back side with a constant multispectral light.

To assess the influence of the grain size and recombination at grain boundaries, on recombination at the back surface, we presented in figure 14 its profile according to the recombination velocity at the grain boundaries for different grain sizes.

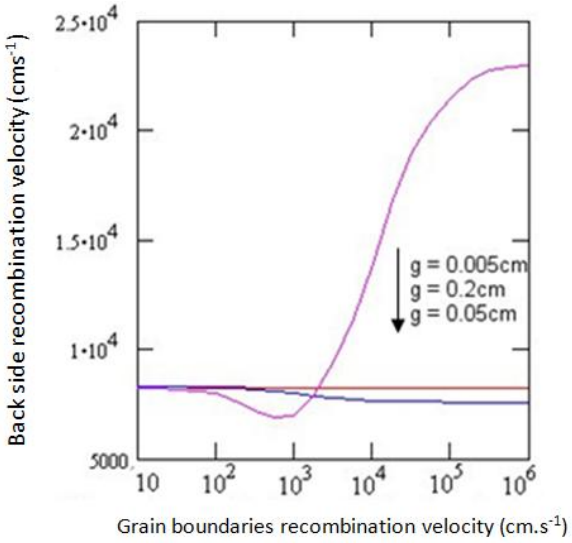

Figure 14: Profile of the recombination velocity at rear side, depending on the recombination velocity at grain boundaries for different grain sizes; $wb=0.03cm$ *and AM1.5*

4. Conclusion

We have shown the influence of g and Sg on the minority charge carrier density. Using the Sf concept, I (Sf) - V (Sf) characteristic has been plotted focusing g and Sg effects. Thus, it could be used to determine series and shunt resistors (Rs, Rsh) and either the transition capacitance Cz

Expression of minority carrier junction recombination velocity on back side (Sb) versus grain size (g) and the grain boundaries recombination velocity (Sg) is established for a given solar cell thickness wb. The calibration curves indicate the interest g and Sg ranges which are of interest for making a solar cell leading to low Sb values (With BSF) with a BSF effect and those giving high Sb values (ohmic contact avoidance).

The solar cell could be studied for a low thickness wb, which would make it possible to bring the carriers closer the junction.

References

[1]. Le Quang Nam M. Rodot. Solar cells with 15.6% efficiency on multicrystalline silicon, using impurity gettering back surface field and emitter passivation. Int. J. Solar Energy, 1992, vol. 11, pp. 273-279.

[2]. S. Martinuzzi, I. Perichad and M. Stemmer. External Gettering around extende defects in multicrystalline silicon wafers. Solid State Phenomena, Vols. 37 – 38 (1994) pp. 361-366

[3]. J. Ducas. 3D Modelling of a Reverse Cell Made with Improved Multicrystalline Silicon Wafer. Solar Energy Materials & Solar Cells, 32, (1994) pp. 71-88

[4]. Kazuhiko Sagara and Eiich Murakami. Effect of grain size on conduction mechanism in polycrystalline silicon. J.Appl. Phys. Lett. 54(20), 15 May 1989, pp 2003-2005

[5]. Ryuichi Shimokawa and Yutaka Hayashi. Effect of localized grain boundaries in semicrystalline silicon solar cell. J.Appl. Phys. 59(7). 1 April 1986, pp 2571-2576

[6]. S.C. Jain. The effective lifetime in semicrystalline silicon Solar Cells, Vol. 9, Pp 345-352, (1983)

[7]. S. M. Davidson. Injection and doping dependence of sem and scanning light spot diffusion length measurements in silicon power rectifiers. Solid-State Electronics, Vol. 25, N°4, (1982), pp261-272

[8]. F. Caldararu, M. Caldararu, S. Nan, D. Nicolaescu and S. Vasile. Analytical two-dimensional model of solar cell current-voltage characteristics. Solid-State Electronics, Vol. 34, N°6, (1991), pp553-558

[9]. Jerry G. Fossum and Fredrik A. Lindholm. Theory of grain-boundary and intragrain recombination currents in polysilicon p-n-junction solar cells. IEEE Transactions on electron devices, Vol. ED-27, N°4, (1980),pp.692-699

[10]. Y. L. B. Bocande, A. Correa, I. Gaye, M. L. Sow and G. Sissoko. Bulk and surfaces parameters determination in high efficiency Si solar cells. Renewable Energy, vol 5, part III, pp. 1698-1700, (1994)-Pergamon, 0960-1481
[11]. Nzonzolo, Lilonga-Boyenga, D., Mabika, C.N. and Sissoko, G.(2016). Two-Dimensional Finite Element Method Analysis Effect of the Recombination Velocity at the Grain Boundaries on the Characteristics of a Polycrystalline Silicon Solar Cell. Circuits and Systems, 7, 4186-4200.http://dx.doi.org/10.4236/cs.2016.713344
[12]. J. Dugas and J. Oualid. 3D-Modelling of polycrystalline silicon solar cells. Revue Phys. Appl ,Vol. 22. pp 677-685, (1987).
[13]. H. El Ghitani and S. Martinuzzi. Influence of dislocations on electrical properties of large grained polycrystalline silicon cells. I. Model. J. Appl. Phys., Vol. 66, N°4. Pp 1717-1722, (1989).
[14]. J. Oualid, M. Bonfils, J P Crest G. Mathian H Amzil, J. Dugas, M. Zehaf And S. Martinuzzi. Photocurrent and Diffusion Lengths at the Vicinity of Grain Boundaries (g.b.) in N and P-type Polysilicon. Evaluation of the g.b. Recombination Velocity. Revue Phys. Appl. 17, (1982), pp119-124
[15]. J. Oualid, C. M. Singal. Influence of illumination on the grain boundaries recombination velocity in silicon. J. Appl. Phys. 55(4), 15 feb. (1984), pp 1195-1205.
[16]. S. Mbodji**,** B. Mbow, F. I. Barro and G. Sissoko. A 3D model for thickness and diffusion capacitance of emitter-base junction determination in a bifacial polycrystalline solar cell under real operating condition. Turkish Journal of Physics, 35 (2011), pp.281–29.
[17]. B. Ba, M. Kane, A. Fickou, G. Sissoko. Excess minority carrier densities and transient short circuit currents in polycrystalline silicon solar cells. Solar Energy Materials and Solar cells 31 (1993), 33-49, 0927-0248 /93/$ 06.00 © 1993 êlsevier Science Publishers B. V.
[18]. F. I. Barro, A. Seidou Maiga, A. Wereme and G. Sissoko. Determination of recombination parameters in the base of a bifacial silicon solar cell under constant multispectral light. Physical and Chemical News, 56 (2010), 76-84.
[19]. Luc Bousse, Shahriar Mostarshed and Dafeman. Investigation of Carrier Transport Through Silicon Wafers by Photocurrent Measurements. J. Appl. Phys. 75 (8), (1994), pp4000-4008.
[20]. M. Kunst and A. Sanders. Transport of excess carriers in silicon wafers. Semicond. Sci. Technol. 7 (1992) 51-59 in the UK.
[21]. Avraham Gover and Paul Strella. Vertical Multijunction Solar-Cell One-Dimensional Analysis IEEE Transactions on electron devices, Vol.21, N^{o}6 , (1974), pp.351-356.
[22]. Sudha Gupta, Peroz Ahmed And Suresh Garg. A method for the determination of the material parameters τ, D, L_o, S and a from measured short-circuit photocurrent. Solar Cells, Vol. 25, pp 61-72, (1988)
[23]. Daniel L. Meier, Jeong-Mo Hwang, Robert B. Campbell. The effect of doping density and injection level on minority carrier lifetime as applied to bifacial dendritic Web silicon solar cells. IEEE Transactions on electron devices, vol. ED-3, NO. 1. January (1988), pp. 70-79
[24]. M. M. Dione, H. LY Diallo, M. Wade, I. LY, M. Thiame, F. Toure, A. Gueye Camara, N. Dieme, Z. Nouhou Bako, S. Mbodji, F. I. Barro, G. Sissoko. "Determination of the shunt and series resistance of a vertical multijunction solar cell under constant multispectral light". Proceedings of 26th European Photovoltaic Solar Energy Conference and Exhibition 1CV.3.6 (2011), pp 250-254; http://www.eupvsec-proceedings.com
[25]. S. R. Dhariwal. Photocurrent and photovoltage from polycrystalline p-n junction solar cells. Solar Cells, Vol. 25, pp 223-233, (1988)
[26]. J. Furlan, and S. Amon. Approximation of the carrier generation rate in illuminated silicon. Solid State Electron, 28 (1985) 1241–43.
[27]. S. N. Mohammad. An alternative method for the performance analysis of silicon solar cells. J. Appl. Phys. 61(2) (1987) 767-777.
[28]. M.C. Halder and T.R. Wiliams. Grain boundary effects in polycrystalline silicon solar cells I: Solution of the three dimensional diffusion equation by the green's function method Solar Cells, Vol. 8, Pp 201-223, (1983).
[29]. H. L. Diallo, A. Wereme, A. S. Maïga and G. Sissoko: New approach of both junction and back surface recombination velocities in a 3D modeling study of a polycrystalline silicon solar cell. Eur. Phys. J. Appl. Phys., 42: (2008), pp.203–11.
[30]. B.H. Rose and H.T. Weaver, Determination of effective surface recombination velocity and minority carrier lifetime in high-efficiency Si solar cells", J. Appl. Phys. 54 (1983), 238–247.

[31]. G. Sissoko, E. Nanema, A. Correa, M. Adj, A.L. Ndiaye, M.N. Diarra. Recombination parameters measurement in double sided surface field solar cell. Proceedings of World Renewable Energy Conference, Florence–Italy (1998), pp. 1856–1859.